RESEARCH MEMORANDUM

FREE-FLIGHT PERFORMANCE OF A ROTATING-VANE-SPOILER ROLL CONTROL SYSTEM WITH LOW ACTUATING FORCES

By Eugene D. Schult

Langley Aeronautical Laboratory
Langley Field, Va.

NATIONAL ADVISORY COMMITTEE
FOR AERONAUTICS

WASHINGTON

May 10, 1957

NACA RM L57C21

NATIONAL ADVISORY COMMITTEE FOR AERONAUTICS

RESEARCH MEMORANDUM

FREE-FLIGHT PERFORMANCE OF A ROTATING-VANE-SPOILER ROLL CONTROL SYSTEM WITH LOW ACTUATING FORCES

By Eugene D. Schult

SUMMARY

Free-flight tests of two rocket models were made at Mach numbers between approximately 0.5 and 1.6 to determine the control rolling effectiveness and system operation of an autorotating-vane spoiler on a missile configuration with an 80° delta, cruciform wing. The results indicated that the system operated fairly satisfactorily as a flicker-type roll control except at low supersonic speeds. At these speeds both the rolling effectiveness and the vane-operating torque produced by the free stream were marginally low. The drag of the control was high but of a level expected for spoilers.

INTRODUCTION

The basic need for simplified control systems which require low actuating forces is apparent. A number of devices for control have been advanced to satisfy this need and among these devices is the rotating-vane spoiler (refs. 1 to 3). This spoiler is fundamentally a flicker-type control suitable for missile guidance applications such as proposed in reference 4. The spoiler consists of two vane segments mounted on opposite ends of a rotating shaft passing through the wing normal to the chord plane. The vanes are oriented at right angles to one another and are shaped to provide autorotation. Free autorotation is prevented, however, by an escapement which limits the shaft rotation to increments of one-fourth revolution. Thus the lift or control sense is changed by permitting either the upper or lower vane to face upstream and act as a spoiler. The only energy required of the servomotor is to actuate the escapement.

Previous investigations have determined a vane shape which will provide sufficient torque for autorotation and also have indicated the approximate level of lift and rolling effectiveness to be expected from simple flat plates arranged to simulate a vane spoiler in one control

position (refs. 1 to 3). The purpose of the present investigation was to flight test the integrated control system operating on a missile configuration. Two models were flown - one with vanes fixed in one control position to measure the steady-state roll response, the other with vanes pulsed to alternate control positions to measure the transient response. One fault previously encountered - that of vane rebound off the escapement pin - was corrected on the present configuration.

The flight tests were conducted at the Langley Pilotless Aircraft Research Station at Wallops Island, Va.

SYMBOLS

A_f projected frontal area of vane face, sq ft

b total wing span, ft

C_D total-drag coefficient of configuration, $\frac{\text{Drag}}{qS_{\text{exposed}}}$

C_l rolling-moment coefficient, $\frac{\text{Rolling moment}}{qSb}$

$C_{l,v}$ control rolling-moment coefficient due to vane spoiler

C_{l_p} damping-in-roll derivative, $\frac{\partial C_l}{\partial\left(\frac{pb}{2V}\right)}$

h projected height of spoiler above wing surface, in.

I_X mass moment of inertia of model about longitudinal axis, slug-ft^2

M Mach number

p model rolling velocity, radians/sec

$\dot{p}$ model roll acceleration, $\frac{dp}{dt}$, radians/sec^2

$pb/2V$ wing-tip helix angle, radians

q dynamic pressure, $\frac{1}{2}\rho V^2$, lb/sq ft

ρ	air density, slugs/cu ft
S	total cruciform-wing area projected to model center line, sq ft
t	time, sec
V	forward velocity of model, ft/sec
w_e	projected width of vane edge, in.
y_f	projected length of vane face, in.

MODELS AND TEST TECHNIQUE

Sketches and dimensions of the two models employed in the present investigation are shown in figures 1 and 2. The 80° delta, cruciform wings were of modified hexagonal section, tapering at the trailing edge to one-half maximum thickness. Both models were externally similar except for a 5-inch fuselage extension added at the rear of model 2 and the rounded leading edges (shoulders) of the wing at the body juncture of model 2 (fig. 2). The S-shaped vanes were machined from 2024-T aluminum alloy and located at midexposed span on two of the wings. They were fixed in one control position on model 1. On model 2 the vanes and connecting shafts rotated in plain sleeve bearings and were released to alternate control positions by means of a motor-toggle arrangement which programmed the escapement. The escapement stops were designed to engage the upper and lower vanes alternately; thus, free autorotation of the vanes was restricted to increments of one-fourth revolution. A low-friction ratchet device was incorporated to lock the vanes against the stop after each control pulse to prevent vane rebound and the momentary loss of control observed in the investigation of reference 2.

Photographs of model 1 taken prior to the flight tests are presented as figure 3. The rocket propulsion system (two stage on model 1, one stage on model 2) accelerated the models to the maximum test Mach number in about 3 seconds. The test measurements were made during the following 20 seconds of decelerating flight along the ascending portion of the trajectory. Measurements were made of the model velocity, range, elevation, and azimuth with a CW Doppler velocimeter and an NACA modified SCR-584 radar set. These data, and the radiosonde data permitted an evaluation of the Mach number M and the total-drag coefficient C_D as functions of time.

For model 1 measurements of the rolling velocity p were obtained by means of a spinsonde polarized-wave transmitter within the model and

special rotating-antenna ground receiving equipment (ref. 5). These measurements were used to calculate the wing-tip helix angle.

On model 2 telemetered time histories of vane position, roll acceleration, and stream total pressure were obtained by means of an inductance-type position indicator, a roll accelerometer, and a total pressure probe, respectively. The rolling velocity of the model was determined by the method used for model 1.

The test Reynolds numbers for both flights are presented in figure 4 as a function of Mach number.

DATA REDUCTION

The method for determining the model velocity, Mach number, drag coefficient, and wing-tip helix angles have been described in a previous section. The vane-spoiler rolling-moment coefficient $C_{l,v}$ and model damping-in-roll derivative C_{l_p} were obtained from solutions of the following first-order differential equation which describes the pure rolling motion of the model subject to a control step input:

$$\frac{I_X \dot{p}}{qSb} - C_{l_p}\left(\frac{b}{2V}\right)p = C_{l,v} \tag{1}$$

Solving for the rolling velocity p which is initially some value p_o at t_o when the control is pulsed, gives

$$p = \frac{C_{l,v}}{-C_{l_p}}\left(\frac{2V}{b}\right)\left(1 - e^{-kt}\right) + p_o e^{-kt} \tag{2}$$

where t is the incremental time after t_o and

$$k = \frac{-C_{l_p}}{2}\left(\frac{q}{V}\right)\left(\frac{Sb^2}{I_X}\right)$$

and is the inverse of the model time constant in pure roll. Differentiating equation (2) with respect to time results in an expression for the roll acceleration during that portion of the response history following the step input:

$$\dot{p} = e^{-kt}\left[C_{l,v} + C_{l_p}\left(\frac{p_o b}{2V}\right)\right]\frac{qSb}{I_X} \qquad (3)$$

Semilogarithmic plots of the parameter $\left(I_X\dot{p}/qSb\right)$ against time yield curves of slope k from which values of the damping-in-roll derivative C_{l_p} were obtained by the method of averages outlined in reference 6. These values of C_{l_p} were then substituted into equation (1) to determine the control rolling-moment coefficient $C_{l,v}$.

ACCURACIES AND CORRECTIONS

The test results and measurements are believed to be accurate to within the following limits which have been determined from previous flight experiences:

M	±0.01
C_D	±0.002
pb/2V	±0.002
p, radians/sec	±2
$\dot{p}$, radians/sec^2	±10

The probable errors in rolling-moment coefficient due to vane spoiler and in damping-in-roll derivative are estimated to be of the following order:

$C_{l,v}$	±0.0002
C_{l_p}	±0.003

On model 1 the small tare rolling velocities which result from small variations in wing incidence (from zero) due to construction tolerances were accounted for by means of data from reference 7 and measured values of wing incidence. The method of measuring wing incidence is believed to be accurate to within ±0.002° at the wing mean aerodynamic chord. Measured values of incidence were of the order of ±0.05° and averaged out to approximately 0.014° of roll-causing incidence for model 1. On model 2 the small variations in wing incidence averaged out to approximately zero and were neglected in the data reduction.

Slight corrections were applied to the rolling-effectiveness data (pb/2V) of model 1 to account for the effects of model inertia about the roll axis when the model was subjected to large changes in rolling velocity. It can be shown from equation (1) that this correction for model inertia has the form:

$$\left(\frac{pb}{2V}\right)_{\text{steady state}} = \left(\frac{pb}{2V}\right)_{\text{meas}}\left(1 + \frac{I_X\dot{p}}{M_d}\right) \qquad (4)$$

where

$$M_d = -C_{l_p}\left(\frac{pb}{2V}\right)_{\text{meas}} qSb$$

and is the damping moment due to rolling at the measured value of (pb/2V). Figure 5 presents the variation of rolling effectiveness of model 1 with Mach number and shows the magnitude of the correction to the steady-state condition.

RESULTS AND DISCUSSION

The test results are presented in figures 5 to 8. Figure 5 presents the effect of Mach number on the zero-lift rolling effectiveness of the vane spoiler fixed in one control position. These results indicate abrupt losses in rolling effectiveness in the transonic range. The region of near-zero spoiler effectiveness near Mach number 1.2 was unexpected because it was not observed in the data of reference 2 for a configuration with 60° delta wings undergoing lift.

In figure 6 time histories of the control position, roll acceleration, rolling velocity, dynamic pressure, and Mach number are presented for a portion of the flight of model 2. A region of vane ineffectiveness is noted at the top of the figure where apparently the vane torque was insufficient to overcome friction in the plain sleeve bearings and the vane locking device. As a result the vanes were unable to rotate and engage the stops properly over a small Mach number range near 1.2. Data of reference 3 for a nearly similar vane at a Mach number of 1.2 show some variations in vane torque with vane rotation but no regions of complete torque ineffectiveness. The use of ball bearings on the vane shaft may therefore be helpful in reducing shaft friction and possibly eliminating the range of vane ineffectiveness.

The time lag for the vanes to rotate 90° and reverse control sense was of the order of 0.03 second throughout the flight Mach number range. In several instances and for unknown reasons one vane was released late as shown in figure 6 at 8.4 seconds. This late release caused some delay in attaining the maximum rolling moment and also what is believed to be pitching oscillations of the model because in this small time interval the spoilers act effectively as a pitch control. These oscillations in angle of attack were detected in the drag data and adversely affected the roll response to that particular control pulse. The data for these

delayed-release pulses were not used in the calculations of moment coefficients.

Figure 7 presents variations of calculated values of the damping-in-roll derivative and spoiler rolling-moment coefficient with Mach number. One C_{l_p} point is shown for each pulse and these values are compared with other data (refs. 8 and 9) and with slender wing-body theory (ref. 10). The basic model configuration of reference 8 was the same as that of model 1 in this investigation except for small inlet stores attached to the wing tips. Reference 9 includes data from flight models with delta cruciform wings swept back 45°, 60°, and 70°. Cross plots of C_{l_p} against sweep angle yield the flight-data curve shown in figure 7. (It is assumed that $C_{l_p} = 0$ at 90° sweep.) Aside from the unexplained loss in damping at transonic speeds, the present results compared favorably with the other data and theory.

Calculated values of the spoiler rolling-moment coefficients are shown in the lower plot (fig. 7). The three data points shown for each pulse are distinguished symbolically from the data of adjacent pulses. The midpoints in each case are representative of data taken near zero rolling velocity, whereas the high points are generally nearer the final values of rolling velocity. The curve was calculated by means of the following equation:

$$C_{l,v} = \left(-C_{l_p}\right)\left(pb/2V\right)_{\text{steady state}} \tag{5}$$

In this equation the corrected helix-angle data of model 1 (fig. 5) and slender-wing-body-theory values of C_{l_p} (ref. 10) were used. The observed scatter of data points is believed to be primarily due to inaccuracies in the measuring technique.

Figure 8 presents the measured drag coefficients for the models and their components. The oscillations in drag are believed to be largely due to the pitch oscillations of the model resulting from the delayed release of one vane. The slightly higher drag level of model 2 was expected because of the presence of a total pressure probe, rounded leading edges (shoulders) of the wing at the body juncture, and a rougher model-surface finish caused by unfilled screw-head indentations. A comparison of curves shows that placing spoilers on 2 of the 4 panels effectively doubled the incremental drag of the cruciform wing throughout the speed range. This drag increase is of the same order as that obtained with other types of spoilers on this same wing-body combination (ref. 7).

CONCLUDING REMARKS

The results of free-flight tests of an autorotating-vane-spoiler roll-control system with potentially low servomotor requirements in the Mach number range between approximately 0.5 and 1.6 indicates that the system operated fairly satisfactorily except at low supersonic speeds. At these speeds a combination of low rolling effectiveness and low-vane torque resulted in marginal control. The drag of the control was high but of a level expected for spoilers.

Langley Aeronautical Laboratory,
National Advisory Committee for Aeronautics,
Langley Field, Va., March 7, 1957.

[redacted]

REFERENCES

1. Curfman, Howard J., Jr., Strass, H. Kurt, and Crane, Harold L.: Investigations Toward Simplification of Missile Control Systems. NACA RM L53I21a, 1953.

2. Schult, Eugene D.: A Free-Flight Investigation at High Subsonic and Low Supersonic Speeds of the Rolling Effectiveness and Drag of Three Spoiler Controls Having Potentially Low Actuating-Force Requirements. NACA RM L55G11a, 1955.

3. Wiley, Harleth G., and Hayes, William C., Jr.: Wind-Tunnel Investigations at Low and Transonic Speeds of the Feasibility of Self-Actuating Spoilers as a Lateral-Control Device for a Missile. NACA RM L53K27, 1954.

4. Gardiner, Robert A.: A Combined Aerodynamic and Guidance Approach for a Simple Homing System. NACA RM L53I10a, 1953.

5. Harris, Orville R.: Determination of the Rate of Roll of Pilotless Aircraft Research Models by Means of Polarized Radio Waves. NACA TN 2023, 1950.

6. Lipka, Joseph: Graphical and Mechanical Computation. John Wiley & Sons, Inc., 1918.

7. Schult, Eugene D.: Free-Flight Investigations at Mach Numbers Between 0.5 and 1.7 of the Zero-Lift Rolling Effectiveness and Drag of Various Surface, Spoiler, and Jet Controls on an 80° Delta-Wing Missile. NACA RM L56H29, 1956.

8. Turner, Thomas R., and Vogler, Raymond D.: Wind-Tunnel Investigation at Transonic Speeds of a Jet Control on an 80° Delta-Wing Missile. NACA RM L55H22, 1955.

9. Sanders, E. Claude, Jr.: Damping in Roll of Models With 45°, 60°, and 70° Delta Wings Determined at High Subsonic, Transonic, and Supersonic Speeds With Rocket-Powered Models. NACA RM L52D22a, 1952.

10. Adams, Gaynor J., and Dugan, Duane W.: Theoretical Damping in Roll and Rolling Moment Due to Differential Wing Incidence for Slender Cruciform Wings and Wing-Body Combinations. NACA Rep. 1088, 1952.

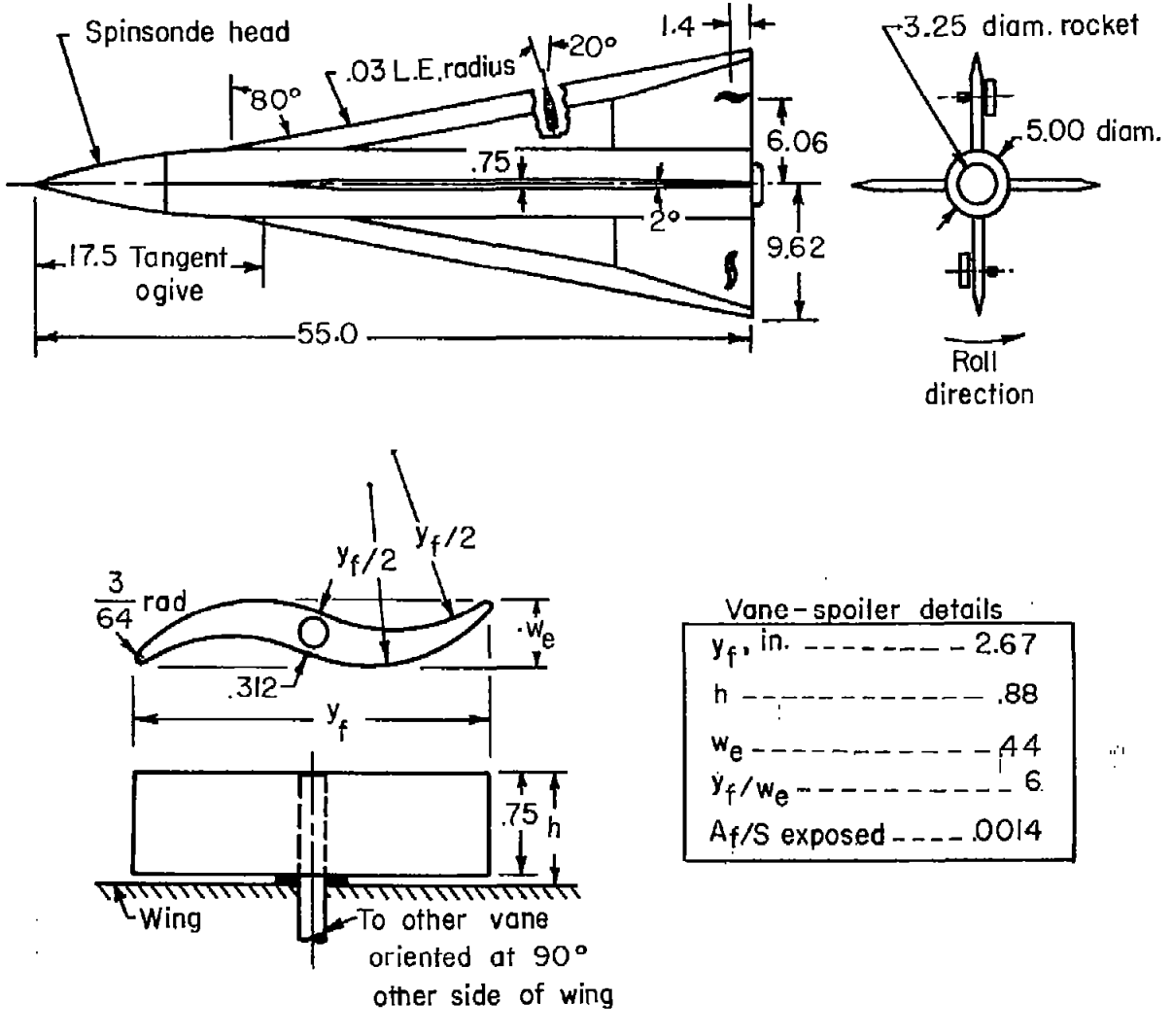

Figure 1.- Details of model 1 with fixed vane-spoiler roll control. All dimensions are in inches unless otherwise indicated.

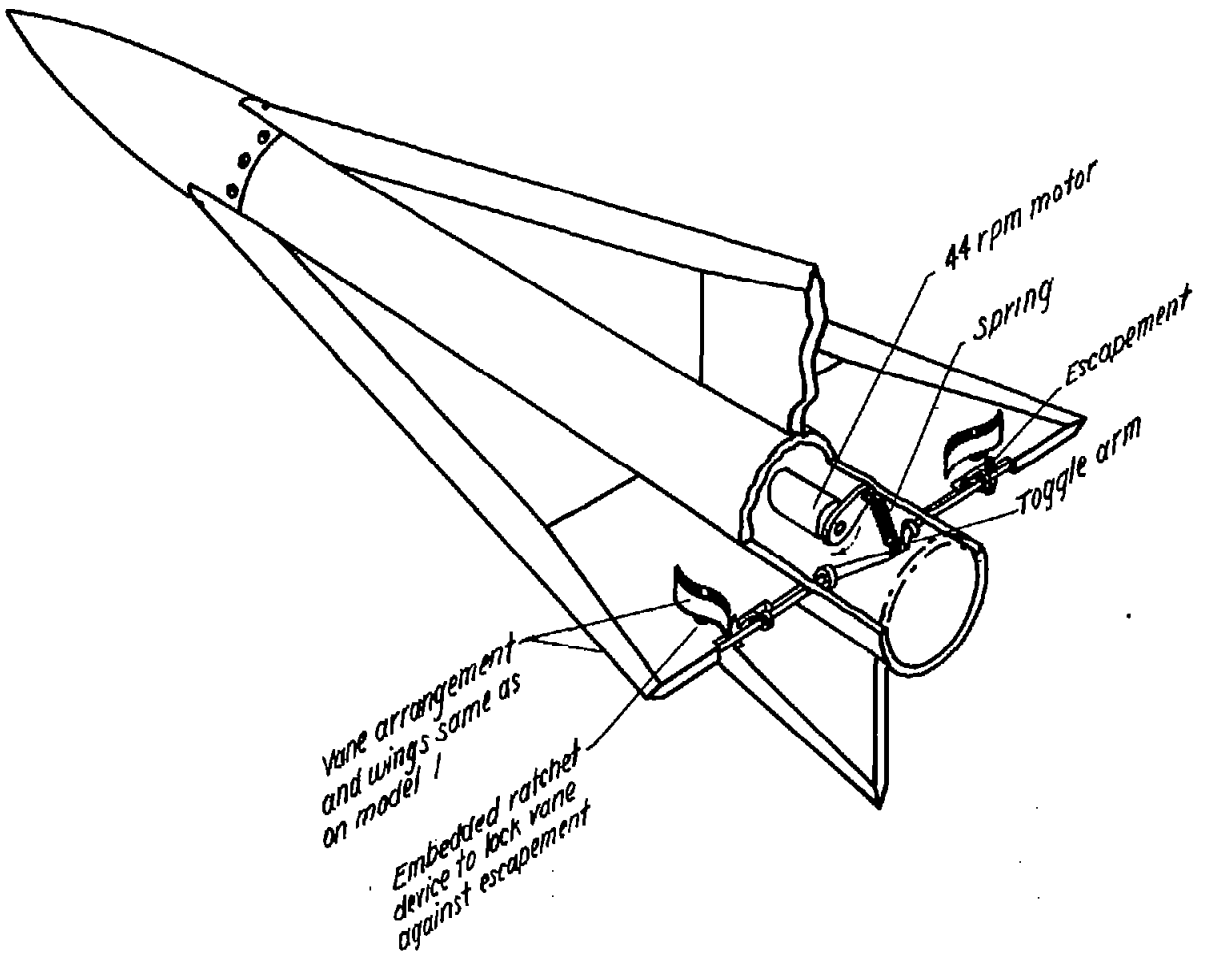

Figure 2.- Sketch of model 2 showing rotating vane spoilers, the vane release escapement, and toggle mechanism employed to pulse the control.

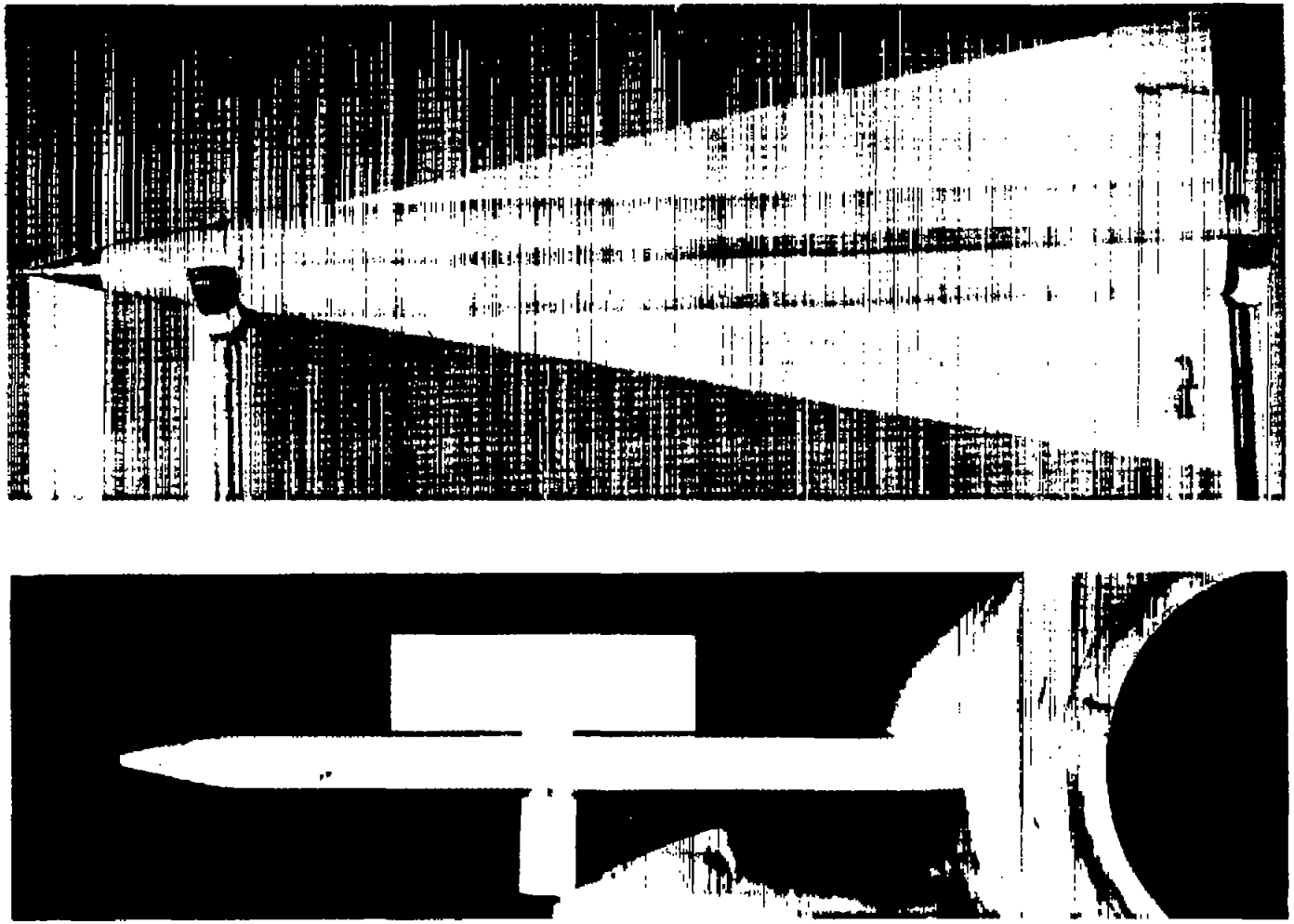

(a) Top and closeup rear views of model 1 with fixed vanes. L-57-181

Figure 3.- Model 1 and booster rocket used in the investigation.

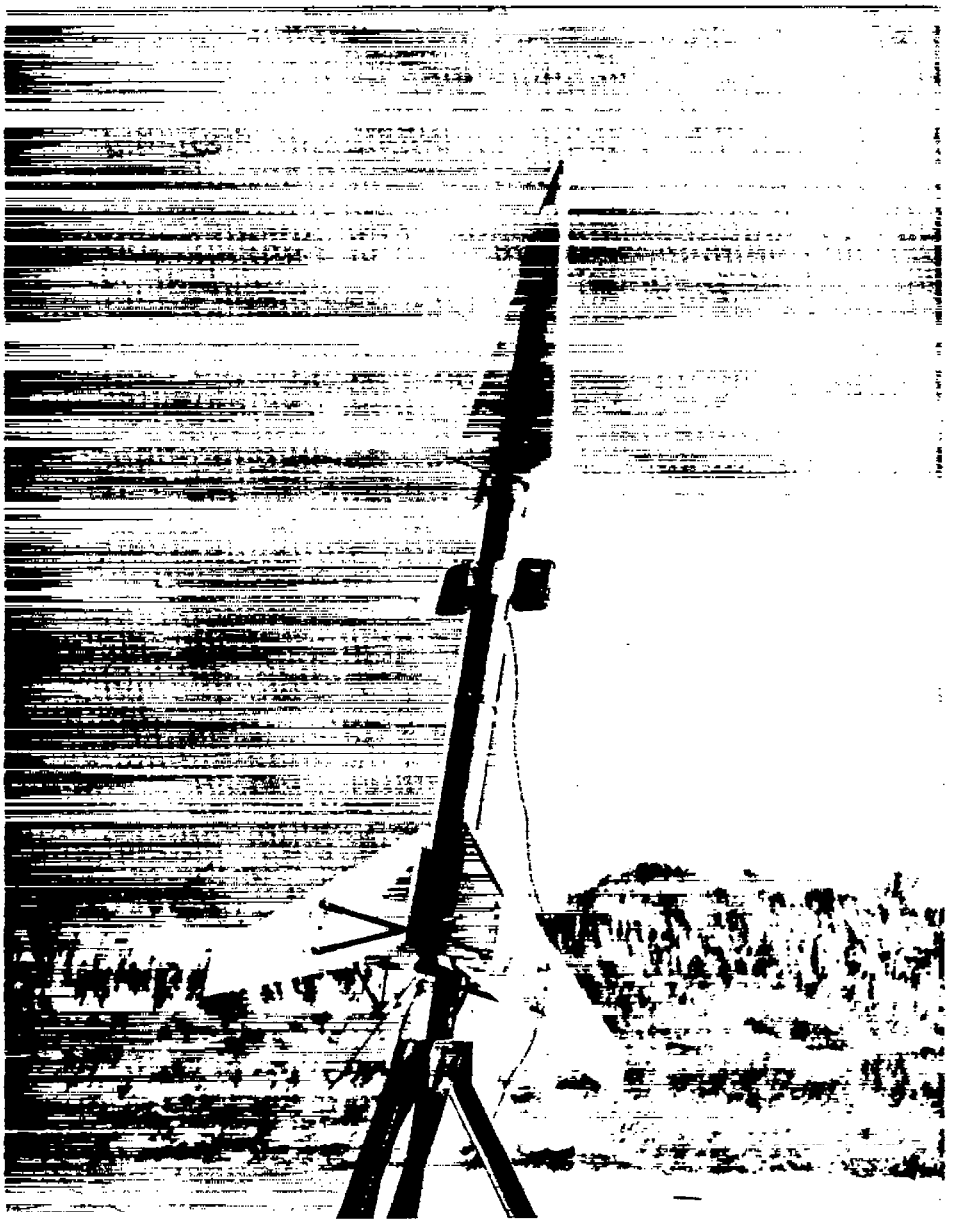

(b) Model 1 and booster rocket on rail launcher. L-87283.1

Figure 3.- Concluded.

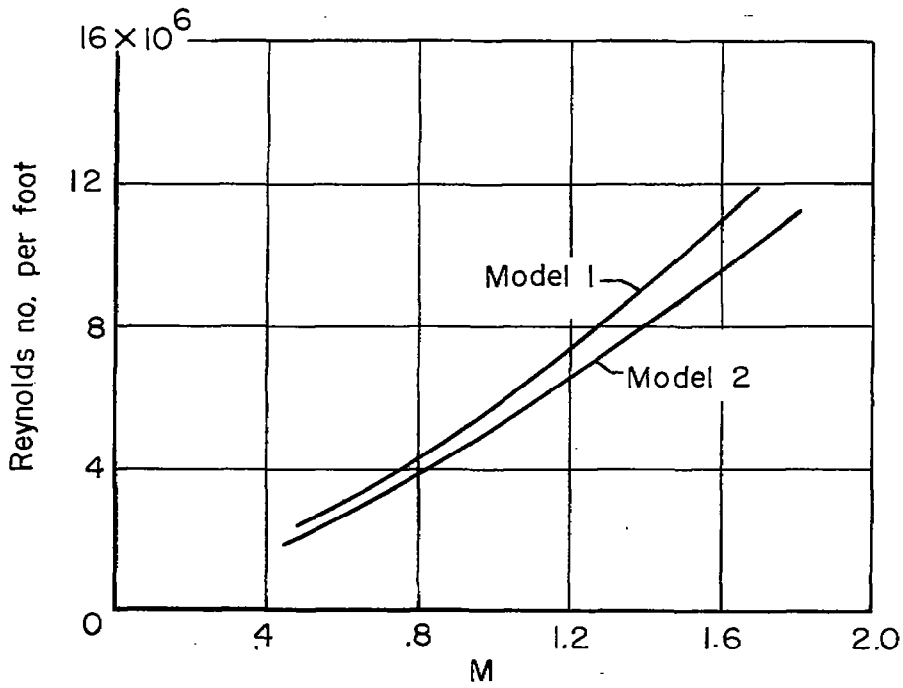

Figure 4.- Variation of test Reynolds number with Mach number for free-flight models.

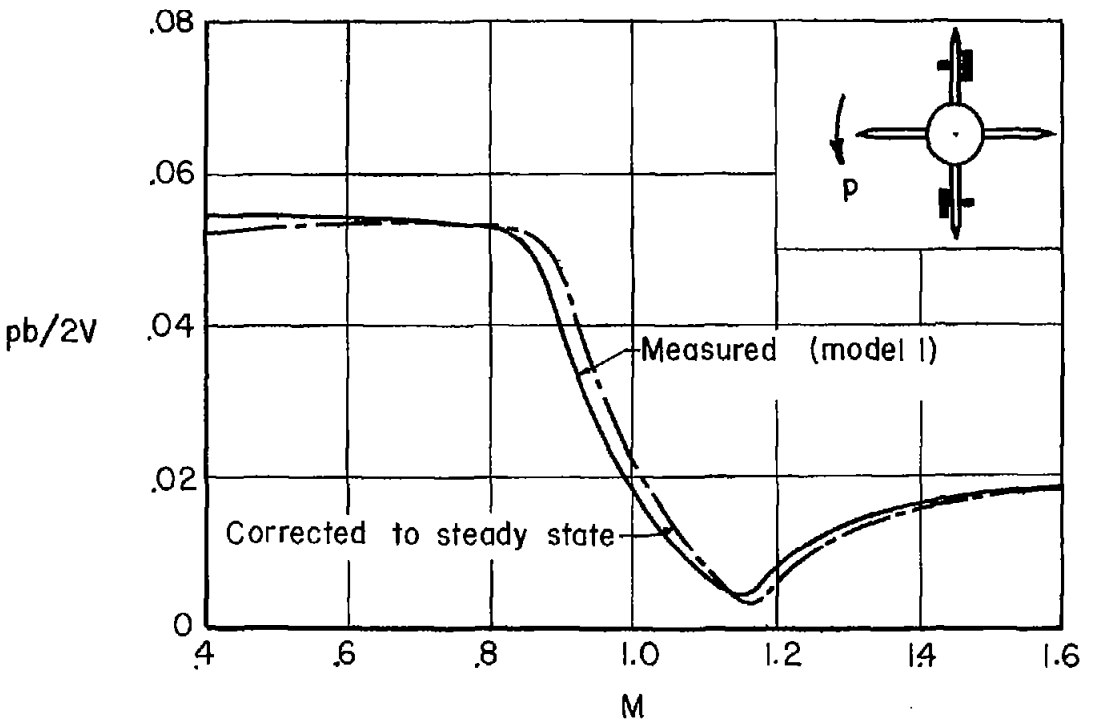

Figure 5.- Variation of zero-lift rolling effectiveness with Mach number for vane spoiler fixed in one control position on model 1.

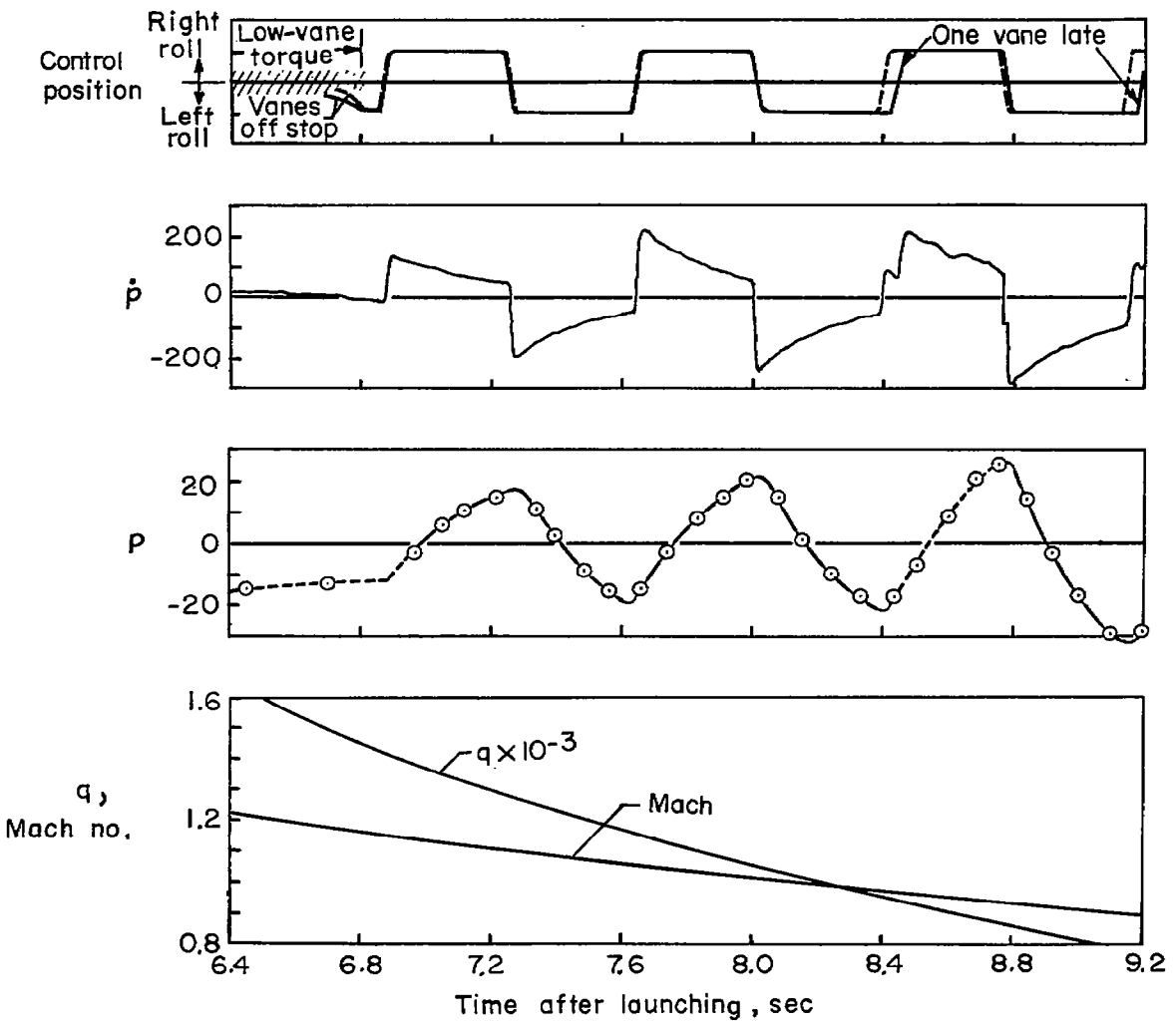

Figure 6.- Roll-response history of model 2 in the transonic speed range.

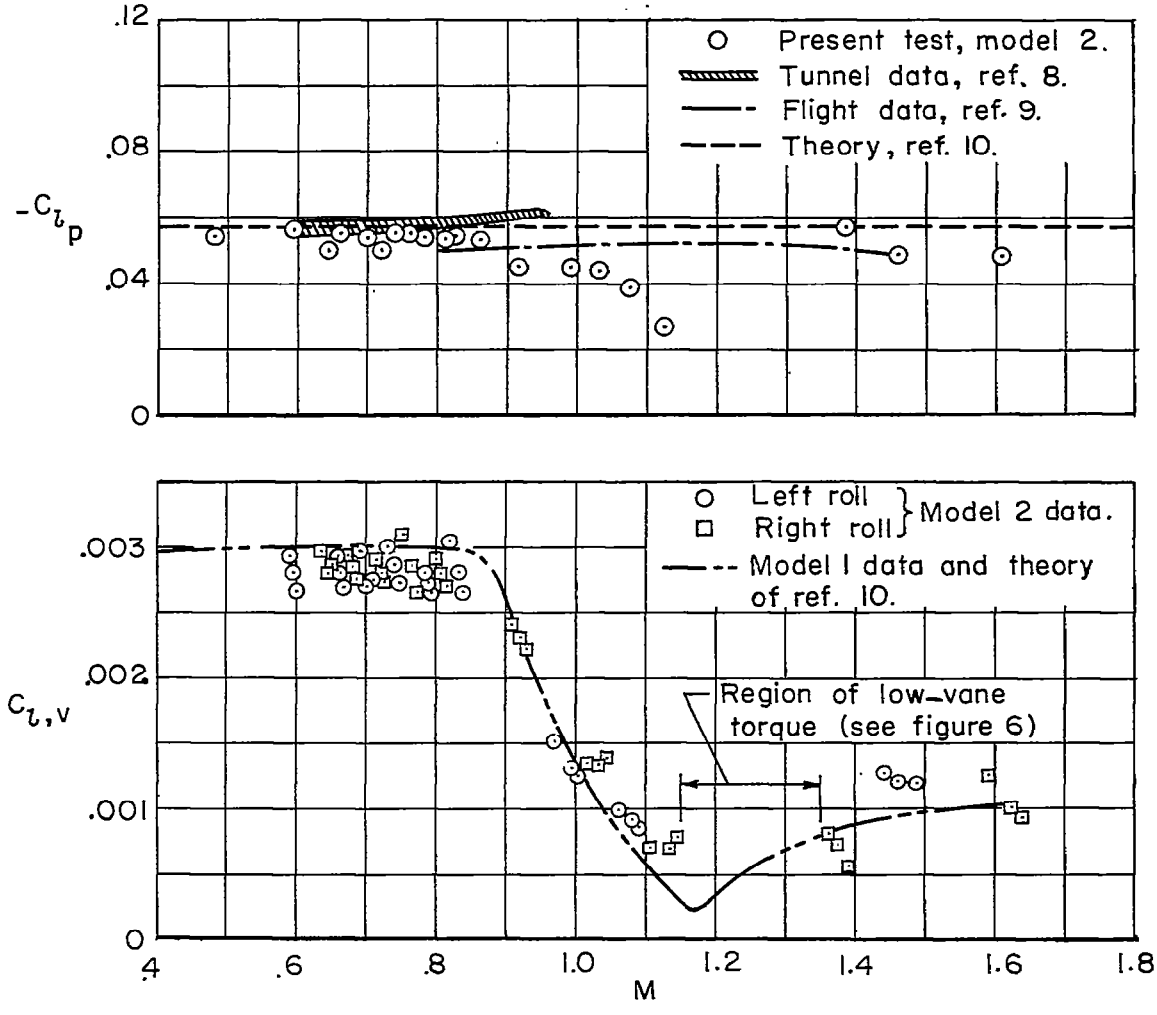

Figure 7.- Variation with Mach number of damping-in-roll derivative and vane rolling-moment coefficient for test configurations. (Coefficients are based on total area of cruciform wings with two vane-spoiler controls.)

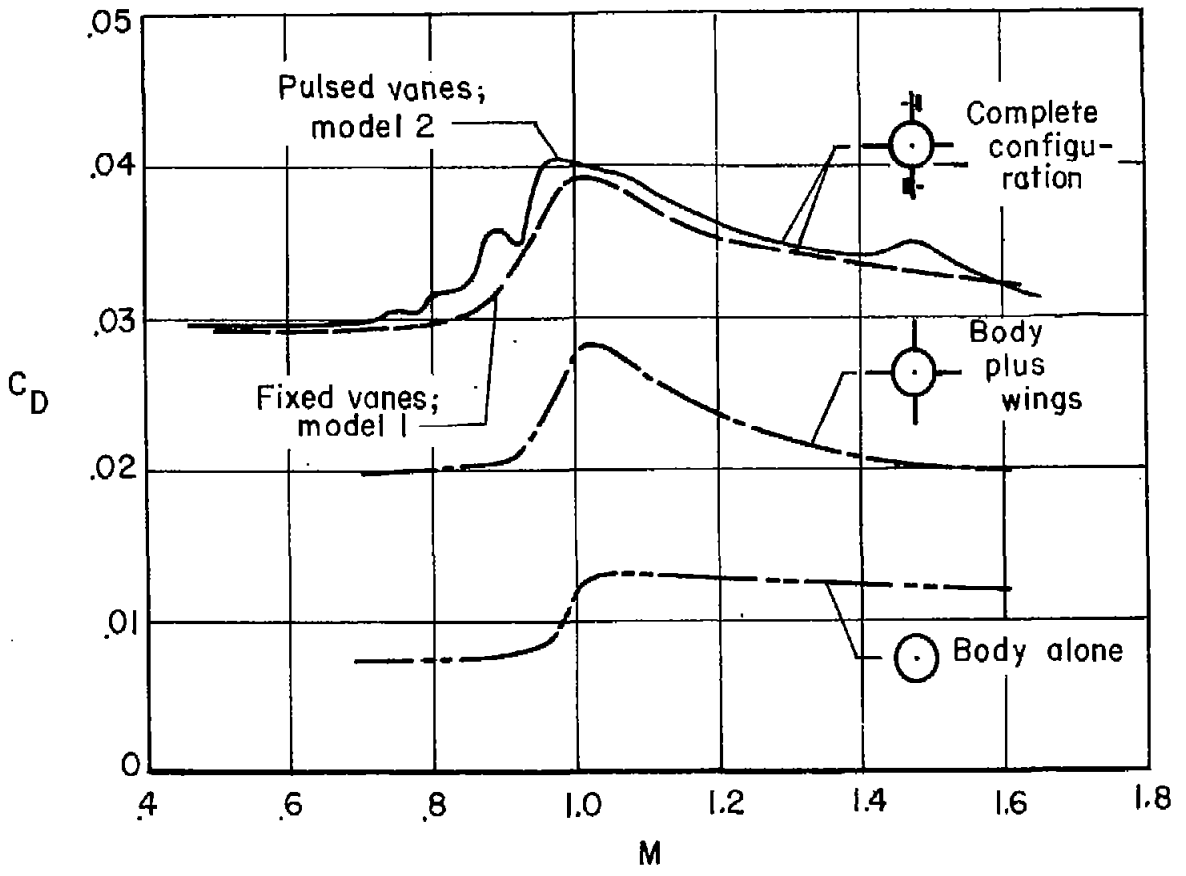

Figure 8.- Drag breakdown of vane-spoiler models. (Drag coefficients are based on exposed wing area; data are from present tests and ref. 7.)